

Spectroscopic detection and characterization of cyanooxomethylum, NCCO^+

Marcel Bast,[†] Julian Böing,[†] Thomas Salomon,[†] Eline Plaar,[†] Igor Savić,[‡]
Mathias Schäfer,[¶] Oskar Asvany,[†] Stephan Schlemmer,[†] and Sven Thorwirth^{*,†}

[†]*I. Physikalisches Institut, Universität zu Köln, Zülpicher Str. 77, 50937 Köln, Germany.*

[‡]*University of Novi Sad, Faculty of Sciences, Department of Physics, Novi Sad 21000, Serbia*

[¶]*Institute of Organic Chemistry, Department of Chemistry, University of Cologne,
Greinstraße 4, 50937 Köln, Germany*

E-mail: sthorwirth@ph1.uni-koeln.de

Abstract

Cyanooxomethylum, NCCO^+ , a fundamental linear acylium ion, has been observed spectroscopically for the first time using action spectroscopy in ion trap apparatuses. A first low-resolution infrared spectrum was obtained between 500 to 1400 cm^{-1} and 2000 to 2500 cm^{-1} using the Free Electron Laser for Infrared eXperiments (FELIX) and the FELion apparatus, employing infrared predissociation of the weakly bound $\text{NCCO}^+ - \text{Ne}$ complex. Subsequently, high-resolution studies of the bare ion were performed with the COLtrap II setup, one targeted at the CN-stretching mode ν_2 around 2150 cm^{-1} using leak-out spectroscopy and one at the pure rotational spectrum employing a leak-out infrared/millimeter-wave double resonance approach covering transition frequencies as high as 246 GHz. Spectroscopic detection and analysis were guided by high-level quantum-chemical calculations performed at the CCSD(T) level of theory.

The collected data permit accurate frequency predictions to support future astronomical searches with sensitive radio telescopes.

Introduction

More than 350 molecules have been detected in space to date and their number continues to grow¹. About 50 of those species are molecular ions that are both positively and negatively charged. A particularly attractive group of ions that has recently triggered astrochemical interest is the group of so-called acylium ions, positively charged species of the general formula $R\text{--CO}^+$. The prototypical formylium ion, $\text{H}\text{--CO}^+$ (aka protonated carbon monoxide) has been known in space for more than 50 years^{2,3} and also was the first polyatomic ion to be detected there. However, it was not until very recently that two other acylium ions were observed by their rotational spectra toward Taurus molecular cloud 1 (TMC-1) in the radio regime: linear $\text{H}\text{--C}\equiv\text{C}\text{--C}\equiv\text{O}^+$,⁴ as well as $\text{CH}_3\text{--C}\equiv\text{O}^+$,⁵ a prolate symmetric rotor. To date, these three species also remain the only acylium ions studied at high spectral resolution in the laboratory.^{4–6} Consequently, high-resolution spectroscopic studies of other simple acylium ions are very desirable to check for their astronomical presence in molecular clouds and to evaluate the astrochemical relevance of acylium ions from a more general perspective.

In the present paper, both low- and high-resolution spectroscopic investigations of a hitherto spectroscopically not known acylium ion will be presented, linear tetratomic cyanooxomethylium, $\text{N}\equiv\text{C}\text{--C}\equiv\text{O}^+$. Despite a number of theoretical studies performed over the years^{7–12} the only experimental characterization of NCCO^+ appears to be that of McGibbon et al. reporting on the presence of NCCO^+ in mass spectra of pyruvonitrile (acetyl cyanide, $\text{CH}_3\text{C}(\text{O})\text{CN}$) and methyl cyanoformate ($\text{CH}_3\text{OC}(\text{O})\text{CN}$).⁸ In the present investigation, selected spectroscopic properties of NCCO^+ have been studied in some detail. Low-resolution

¹An up-to-date list of astronomically detected molecules with complementary information is maintained at the Cologne Database for Molecular Spectroscopy (CDMS)¹ accessible online at <https://cdms.astro.uni-koeln.de/>

infrared (IR) spectra were obtained via predissociation of its weakly bound complex with Ne followed by high-resolution leak-out spectroscopy (LOS) of the ν_2 vibrational fundamental at 2150 cm^{-1} . Finally, the pure rotational spectrum was observed employing a leak-out (LO) infrared/millimeter-wave double resonance (DR) scheme. The spectroscopic findings and analyses, along with results from complementary high-level quantum-chemical calculations, will be summarized in the following.

Experimental methods

Spectroscopic studies of NCCO^+ were performed over the course of three consecutive measurement campaigns using two of our cryogenically cooled 22-pole ion trap apparatus. Experimental setups and the applied action spectroscopic methods are described in some detail in the following.

The first spectroscopic detection of NCCO^+ ions was achieved using the cryogenic 4 K 22-pole ion trap apparatus FELion in combination with the Free Electron Laser for Infrared eXperiments (FELIX) at Radboud University (Nijmegen, The Netherlands).¹³ The experimental setup and typical experimental conditions have been described in detail elsewhere previously.¹⁴ Briefly, NCCO^+ ($m/z = 54$) was generated in a radio frequency (RF) storage ion source (SIS) by electron bombardment of commercially available pyruvonitrile ($\text{CH}_3\text{C}(\text{O})\text{CN}$) using an electron energy of about 55 eV. After mass selecting the pulsed ion beam for $m/z = 54$ in the first quadrupole mass filter (QP I), the ions were trapped in the 22-pole ion trap¹⁵ and cooled down to a nominal temperature of about 7 K using a short pulse of a 3:1 mixture of He:Ne. In such an environment, kinetically and internally cooled ions can form weakly bound ion–Ne complexes through three-body collisions with the noble gas atoms. After trapping times of 1 to 4 s, the trap content was analyzed with a second quadrupole (QP II) and a Daly-type detector. Initially, more than 100,000 NCCO^+ ions were trapped per measurement cycle and found to form $\text{NCCO}^+–\text{Ne}$ complexes

($m/z = 74$) with an efficiency of about 20%. A corresponding mass spectrum is shown in the Supporting Information (Figs. S1 - S2). To record infrared predissociation (IRPD) spectra of the NCCO^+ -Ne weakly bound complex, the ion trap content was irradiated with pulsed IR radiation of the free electron laser at a repetition rate of 10 Hz and with energies of up to a few tens of mJ per pulse. For the IRPD scheme used here, the number of singly tagged ions ($m/z = 74$, mass selected via QP II) is continuously monitored while FELIX is tuned. In case the photon energy matches the excitation energy of a vibrational mode of the cluster, the latter dissociates, which leads to the IRPD spectrum, recorded as a depletion of the ion signal.

High-resolution observations of rotational-vibrational spectra were subsequently performed using the COLtrap II ion trap apparatus,¹⁶ which was recently upgraded to also enable millimeter-wave measurements (Fig. 1). These measurements were performed using LOS,¹⁷ allowing to record IR spectra of bare ions rather than those of weakly bound clusters. In this action spectroscopy scheme, the internal vibrational energy of excited ions is partially converted into kinetic energy of the ions and a neutral collision partner (here N_2), allowing the target ion to overcome the barrier of the exit potential of the ion trap and be detected. In these high-resolution experiments, NCCO^+ ions were produced from methyl cyanoformate ($\text{CH}_3\text{OC(O)CN}$) using an electron energy of about 65 eV (for a mass spectrum see Figs. S3 - S4), mass selected in QP I (see Fig. 1) and injected into the 22-pole ion trap. The nominal trap temperature was kept at 42(2) K to avoid freeze-out of N_2 , which was continuously introduced into the trap at a number density on the order of 10^{12} cm^{-3} . An additional initial helium pulse ($\sim 10^{15} \text{ cm}^{-3}$) was used for efficient trapping and cooling. High-resolution leak-out spectroscopy was performed around 2150 cm^{-1} in the CN-stretching region of NCCO^+ with a narrow line width quantum cascade laser (QCL, Daylight Solutions MHF 1961 - 2205 cm^{-1} , 200 mW) using an irradiation time of about 400 ms per trapping cycle. For wavenumber calibration, a small portion (5%) of the infrared radiation is coupled into a wavemeter (WM, Bristol Instruments, 771A-MIR, quoted accuracy 10^{-3} cm^{-1})

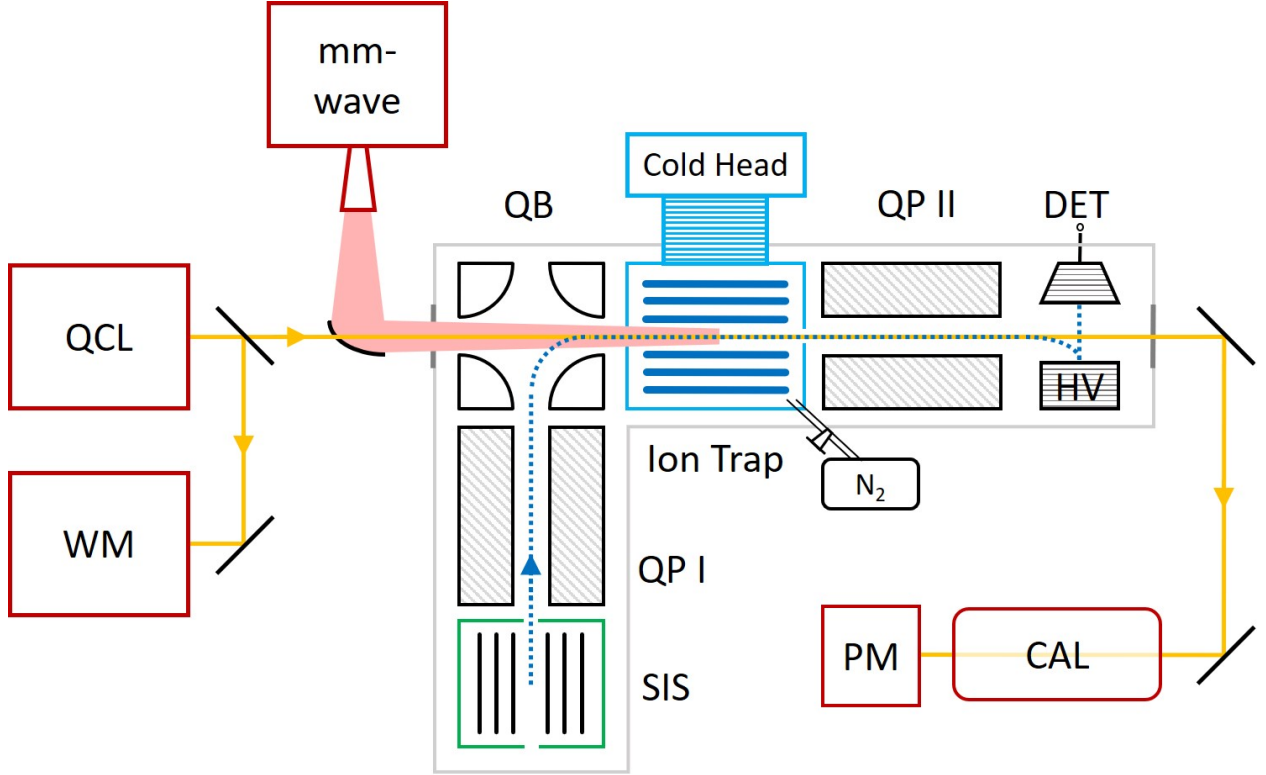


Figure 1: Schematic view of the 10 K 22-pole ion trap apparatus COLtrap II (adapted from Figure 1 in Ref.¹⁶; reproduced with permission from Elsevier). The setup is extended here by a millimeter-wave (mmw) setup for IR/mmw double resonance experiments, consisting of a synthesizer, an amplifier-multiplier chain and a horn antenna. The mmw beam (shown in pale red) is focused by an elliptical mirror and enters the vacuum chamber through a diamond window. A small hole in this mirror also allows the IR laser (shown in yellow) to pass along the axis. See the text for further details.

via a CaF_2 window acting as a beam splitter. In the spectroscopy scheme used here, the number of ions leaking out of the trap was counted during the trapping time. Along the way to the detector, the ions pass through QP II, which selects ions with $m/z = 54$. An off-resonance background LO rate of about 1% per cycle of the total trap content (around 40,000 NCCO^+ counts per cycle) turned out to provide a high S/N ratio. This procedure results in almost background free ion signals upon excitation of a rotational-vibrational transition. To account for potential drifts of experimental settings during long-time measurements, the wavenumber ($\tilde{\nu}$) dependent experimental counts were normalized according to the background LO rate (BG): norm. signal ($\tilde{\nu}$) = $\frac{\text{Counts}(\tilde{\nu}) - \text{BG}}{\text{BG}}$ (see, Ref. 16).

As the photon energy of a pure rotational transition is too low to drive the LO process, an IR/mmw DR scheme⁶ has been applied in a third measurement campaign to record rotational transitions of NCCO^+ . In this approach, the infrared radiation that drives a selected rotational-vibrational transition is kept fixed on-resonance. Meanwhile, the millimeter-wave (mmw) radiation is tuned in fixed steps of 5 to 10 kHz with the corresponding LO rate being monitored. This allows to search for rotational transitions sharing an energy level with the lower rotational level of the infrared transition. The required microwave radiation is provided by a synthesizer (Rohde & Schwarz SMF 100A) referenced to a 10 MHz rubidium atomic clock and driving an amplifier-multiplier chain (AMC, Virginia Diodes Inc. WR 9.0) which upconverts (x9) it into the millimeter-wave range. An additional frequency doubler is used to extend the accessible frequency range even further, providing frequencies as high as 250 GHz. Focused by a horn antenna and an elliptical mirror ($f = 43.7$ mm¹⁸), the mmw radiation enters the vacuum chamber through a diamond window. The mirror features a central hole through which the IR beam from the QCL can pass and overlap with the mmw-radiation in the ion trap as needed for DR spectroscopy.

Quantum-chemical methods

Several computational studies of NCCO^+ performed at various (lower) levels of theory have been reported in the literature previously, primarily aimed at the calculation of structural parameters, harmonic force fields and energy ordering of structural isomers within the $[\text{2C,N,O}]^+$ family.⁷⁻¹² In the present study, quantum-chemical calculations have been performed at the coupled-cluster singles and doubles (CCSD) level augmented by a perturbative treatment of triple excitations, CCSD(T),¹⁹ together with correlation consistent (augmented) polarized valence and (augmented) polarized weighted core-valence basis sets, i.e., cc-pV X Z,²⁰ aug-cc-pV X Z,²⁰⁻²² cc-pwCV X Z,^{20,23} and aug-cc-pwCV X Z^{20,21,23} (with $X=\text{T}$, Q) as well as atomic natural orbital basis sets ANOX ($X=1,2$).²⁴ Equilibrium geometries

have been calculated using analytic gradient techniques,²⁵ while harmonic frequencies have been computed using analytic second-derivative techniques.^{26,27} For anharmonic computations second-order vibrational perturbation theory (VPT2)²⁸ has been employed and additional numerical differentiation of analytic second derivatives has been applied to obtain the third and fourth derivatives required for the application of VPT2.^{27,29} Usage of the frozen core approximation has been indicated throughout by “fc” while “ae” indicates usage of all electrons in the correlation treatment. All calculations have been performed using the CFOUR program package.^{30,31}

To further improve calculated spectroscopically relevant molecular parameters, scaling factors X_{exp}/X_{calc} (with X being a parameter of choice, e.g., B , D , eQq , $\tilde{\nu}$) may be derived using isoelectronic and isostructural species that are known from experiment (see, e.g., Refs. 4,32–34). For NCCO^+ as a 26 electron system, a sizable number of potentially applicable molecular “calibrators” are available from previous high-resolution spectroscopic studies to the extent that their ground state rotational constant B_0 and centrifugal distortion parameter D_0 are known to high accuracy: NCCN ,³⁵ CNCN ,³⁶ C_3O ,³⁷ C_3N^- ,³⁸ C_4H^- ,³⁹ HC_3N ,⁴⁰ HCCNC ,⁴¹ HC_3O^+ ,⁶ NCCNH^+ ,⁴² HC_3NH^+ ,⁴² and HCCNCH^+ .⁴³ Beyond parameters relevant to the ground vibrational state, cyanogen, NCCN , has been studied in the infrared comprehensively³⁵ such as to serve as a useful calibrator for the vibrational spectrum of NCCO^+ .

Structural information about the weakly bound cluster of NCCO^+ with Ne was derived at the fc-CCSD(T)/aug-cc-pVTZ level of theory using a strategy applied recently on similar complexes of other fundamental molecular ions.^{33,44}

Results and discussion

Structures of NCCO^+ and its weakly bound complex with Ne

The equilibrium structural parameters of NCCO^+ calculated at the CCSD(T) level of theory using a variety of basis sets are collected in Table S1 (see the Supporting Information). At the ae-CCSD(T)/cc-pwCVQZ level of theory, that is known to provide very high quality equilibrium structural parameters for molecules containing first- and second-row atoms,^{45,46} the bond lengths are $r_{\text{N}-\text{C}} = 1.1668 \text{ \AA}$, $r_{\text{C}-\text{C}} = 1.3692 \text{ \AA}$, and $r_{\text{C}-\text{O}} = 1.1163 \text{ \AA}$ and the center-of-mass frame dipole moment is 1.62 D.

The energetically favorable position(s) of Ne with respect to NCCO^+ were determined through calculation of a potential energy map. To do this, the fc-CCSD(T)/aug-cc-pVTZ equilibrium structure of NCCO^+ was kept fixed while the position of the Ne atom was used to sample a $10 \times 6 \text{ \AA}^2$ grid at a spacing of 0.25 \AA and distances ranging from 1.5 to 3.5 \AA about the ion. The potential energy map is shown in Fig. 2 and reveals the global minimum to assume a T-shaped structure. Possibly, a very shallow minimum is observed for a linear arrangement in which Ne is attached to N. For advanced structural refinement, the T-shaped global minimum structure was fully optimized at the fc-CCSD(T)/aug-cc-pVTZ level of theory. As with other Ne-tagged weakly bound clusters, the impact of Ne when binding to NCCO^+ is small: Bond lengths between the tagged and bare variants agree to within $2 \times 10^{-4} \text{ \AA}$ and the deviation to linearity in the cluster does not exceed 0.5° (see Supporting Information). As a consequence of this, Ne-tagging is not expected to influence the vibrational spectrum of NCCO^+ by much. Indeed, from fc-CCSD(T)/aug-cc-pVTZ harmonic force field calculations the tagging-induced shifts are found to not exceed some 3 cm^{-1} (Table 1). At the same theoretical level, an estimate of the bond dissociation energy D_0 yields a value of 1.0 kcal/mol.

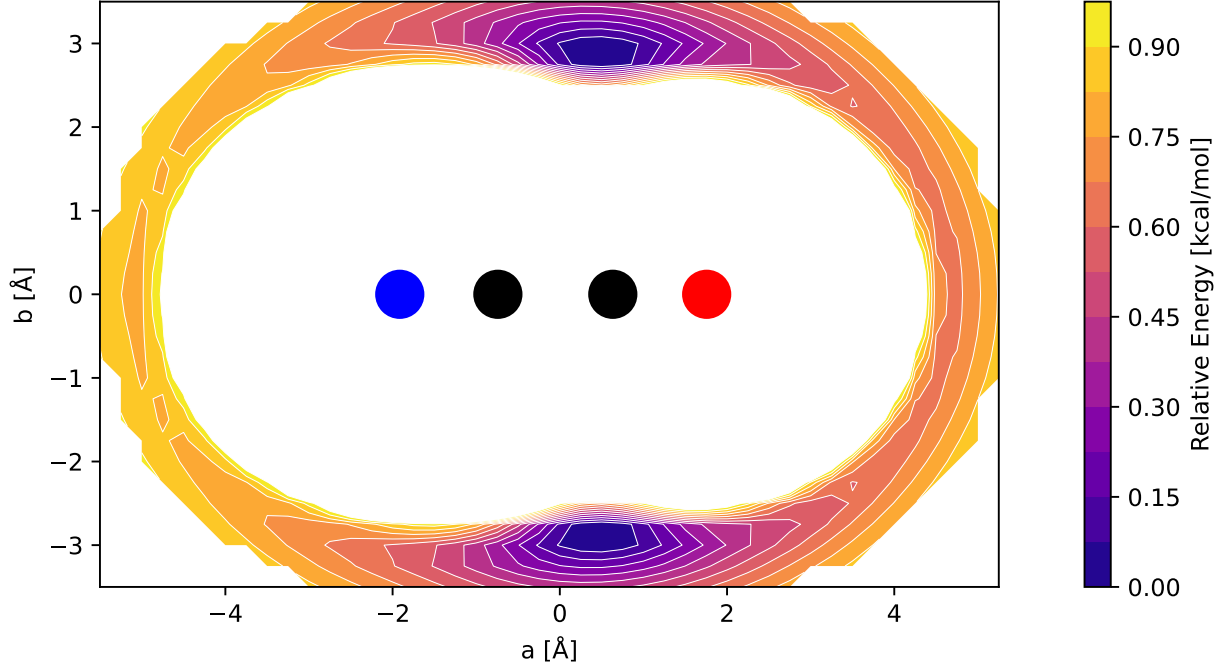


Figure 2: Contour plot of NCCO⁺–Ne showing the fc-CCSD(T)/aug-cc-pVTZ potential energy as a function of the Ne atom position covering the interval [0.075, 0.975] kcal/mol in steps of 0.075 kcal/mol above the global minimum. Atom color code: nitrogen (blue), carbon (black), and oxygen (red).

Table 1: Harmonic vibrational wavenumbers ω_i of bare NCCO⁺ and its T-shaped weakly bound complex with Ne evaluated at the fc-CCSD(T)/aug-cc-pVTZ level of theory (in cm^{-1}).

Mode ^a	NCCO ⁺	NCCO ⁺ –Ne
ω_1	2376	2377
ω_2	2168	2169
ω_3	856	856
ω_4 ^{b,c}	529	527/529
ω_5 ^{b,c}	178	179/181
ω_6 ^d	–	72
ω_7 ^d	–	37

^a Mode index borrowed from untagged NCCO⁺ for the sake of comparability.

^b Doubly degenerate bending mode in linear species.

^c Degeneracy is lifted in the Ne-tagged T-shaped species.

^d Extra low-frequency vibrational modes introduced in the NCCO⁺–Ne complex, arbitrary mode index.

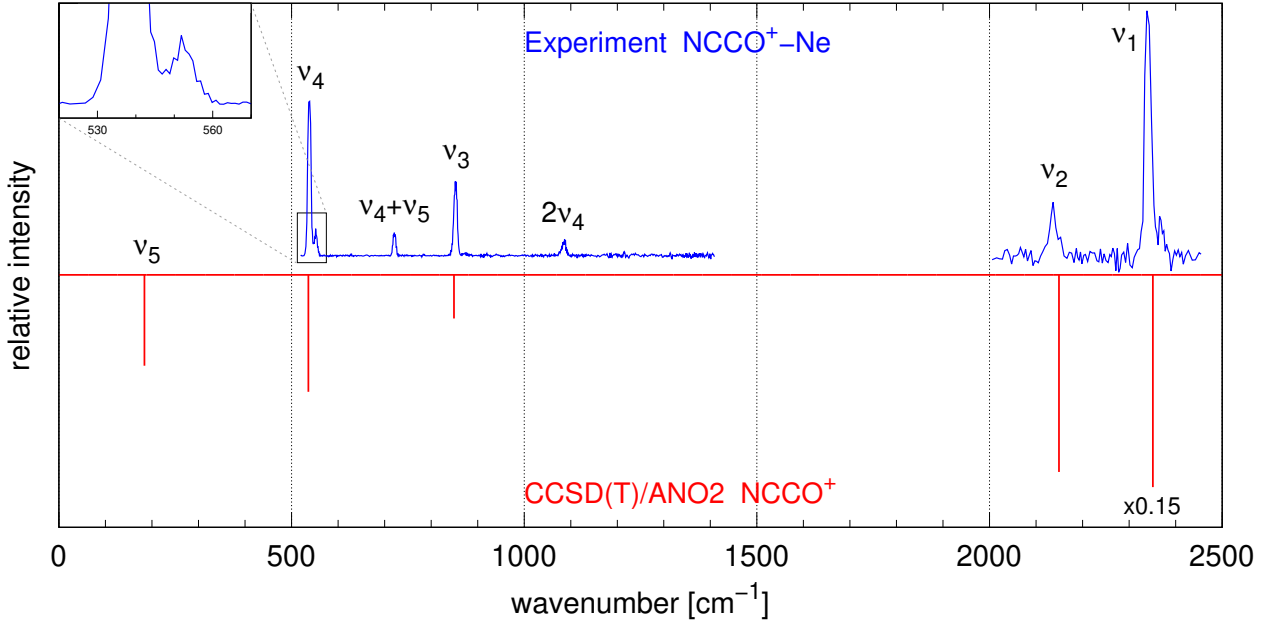


Figure 3: FELIX IRPD spectrum of $\text{NCCO}^+ - \text{Ne}$ (blue trace, top) obtained using the FELion ion trap instrument at a nominal trap temperature of 7 K. Location of the fundamental vibrational bands calculated at the fc-CCSD(T)/ANO2 level of theory is shown as inverted red sticks for comparison.

Broadband IRPD spectrum of $\text{NCCO}^+ - \text{Ne}$

The FELIX IRPD spectrum of $\text{NCCO}^+ - \text{Ne}$ obtained with the FELion apparatus is shown in Fig. 3. During these experiments, two broad regions were covered, one between 500 to 1400 cm^{-1} and another one from 2000 to 2450 cm^{-1} . As a tetratomic linear molecule, NCCO^+ possesses five vibrational fundamentals, three stretching modes and two doubly degenerate bending modes (Table 2). The IRPD spectrum exhibits six features, of which the four most intense can be assigned readily to vibrational fundamentals of NCCO^+ , or more precisely, of NCCO-Ne : the ν_1 -, ν_2 -, and ν_3 -stretching modes and the ν_4 -bending mode, in agreement with anharmonic force field calculations of bare NCCO^+ at the fc-CCSD(T)/ANO2 level (Table 2). The energetically lowest bending mode ν_5 calculated at 184 cm^{-1} was not covered spectroscopically, as were not any fundamental modes related to the Ne-tag which would occur at even lower wavenumbers (Table 1). The ν_4 mode at 538 cm^{-1} , however, shows a weak blue-shifted satellite band at 552 cm^{-1} that might be a combination mode under

participation of Ne; similar features have been observed previously in IRPD spectra of other tagged ions.^{44,47,48} The ν_1 mode of NCCO⁺ might also show such a ‘tag-satellite’.

Table 2: Fundamental vibrational wavenumbers $\tilde{\nu}_i$ of NCCN and NCCO⁺ (in cm^{-1}) and IR band intensities of NCCO⁺ (km/mol) as calculated at the fc-CCSD(T)/ANO2 level of theory.

Mode ^a	NCCN			NCCO ⁺						
	Harm	Anharm	Exp ^b	Mode	Harm	Anharm	BE ^c	Exp ^d	FWHM	Int
$\nu_1(\sigma_g^+)$	2373	2333	2330.49	$\nu_1(\sigma)$	2391	2351	2348	2340(1)	16	440
$\nu_3(\sigma_u^+)$	2186	2155	2157.82	$\nu_2(\sigma)$	2182	2149	2152	2137(1)	20	68
$\nu_2(\sigma_g^+)$	860	840	845.59	$\nu_3(\sigma)$	861	849	855	852(1)	8	22
$\nu_4(\pi_g)$	504	502	502.77	$\nu_4(\pi)$	538	536	537	538(1)	8	39
$\nu_5(\pi_u)$	235	233	233.72	$\nu_5(\pi)$	182	184	185	183(4)*		30
				$2\nu_4(\sigma, \Delta)$				1085(1)	11	
				$\nu_4 + \nu_5(\sigma, \Delta)$				721(1)	7	

^a Ordering of ν_2 and ν_3 bands reversed to match ν_i ordering of NCCO⁺ ($C_{\infty v}$).

^b Experimental vibrational wavenumbers from Ref.³⁵

^c Best estimate (BE) values derived from using NCCN as calibrator, see text for details.

^d Experimental vibrational wavenumbers (and uncertainties) from IRPD of NCCO⁺–Ne complex as derived from Gaussian profile fitting. Typical wavenumber accuracy of FELIX amounts to about 0.5%.

* Estimation from combination band $\nu_4 + \nu_5$ and ν_4 fundamental.

As can also be seen from Table 2, empirical scaling of the fundamental vibrational wavenumbers of NCCO⁺ using isoelectronic NCCN has a minuscule effect only because the calculated and experimental anharmonic vibrational wavenumbers of the latter are very close. Hence, the best estimate (BE) values of NCCO⁺ hardly differ from the unscaled fc-CCSD(T)/ANO2 wavenumbers. The agreement between the experimental and the calculated anharmonic wavenumbers/best estimate (BE) of $\tilde{\nu}_i$ is remarkable (Table 2) as deviations are well within the experimentally observed Full Width at Half Maximum (FWHM) of the bands. The largest discrepancy is observed for the ν_2 fundamental but still amounts to some 12 to 15 cm^{-1} or 0.6 to 0.7% only which is comparable to the typical FELIX wavenumber accuracy of about 0.5%. Actually, in the absence of any high-level force field calculations, spectroscopic assignment of the NCCO⁺ IRPD spectrum would have been feasible rather effortlessly by direct comparison against the NCCN vibrational wavenumbers alone³⁵ taking into account that in a $C_{\infty v}$ species such as NCCO⁺ all vibrational modes are infrared active.

Finally, the two weaker features at 721 cm^{-1} and 1085 cm^{-1} are assigned to the $\nu_4 + \nu_5$

combination band and the $2\nu_4$ overtone, respectively, in good agreement with anharmonic force field predictions. From the former, the ν_5 wavenumber can be estimated by subtraction as $\sim 183\text{ cm}^{-1}$, in very good agreement with the calculated value (Table 2).

High-resolution leak-out spectrum

As a linear species with an ordinary ${}^1\Sigma$ electronic ground state, at high spectral resolution, any stretching vibrational fundamental of NCCO^+ will decompose into characteristic P - and R -branches comprising roughly equally spaced rotational-vibrational transitions governed by the $\Delta J = \pm 1$ selection rule. Guided by the experimental low-resolution IRPD spectrum (Fig. 3) and the high-level force field calculations (Table 3) the high-resolution IR spectrum of NCCO^+ was targeted using the ion trap apparatus COLtrap II.¹⁶ First lines were detected at about 2140 cm^{-1} and spectroscopic assays showed these to belong to the P -branch tail at comparably high rotational quantum numbers (Fig. 4). Scanning upwards, transitions were covered one after another until the ν_2 band center was finally identified at about 2150 cm^{-1} in very good agreement with the high-level calculation and best-estimate values and blueshifted by about 13 cm^{-1} from the IRPD value (Table 2).

Overall, 70 rotational-vibrational lines were finally observed in the wavenumber range from 2138 to 2160 cm^{-1} covering $P(35)$ to $R(34)$. The resulting high-resolution LO spectrum is depicted in Fig. 4. A complete list of the ν_2 transition wavenumbers is provided in the Supporting Information. Generally, the transitions are found to exhibit Gaussian line shapes with an average FWHM of about 0.002 cm^{-1} , see inset in Fig. 4, and intensities that are well described by an absorption spectrum with a rotational temperature of about 50 K (cf., Fig. S6). This suggests that there is no influence of the rotational state on the leak-out process. For a more detailed discussion consult the Supporting Information.

As seen in Fig. 4, the ν_2 spectrum is clean and apparently void of lines from other (hot or combination) bands. Spectral line fitting was performed throughout using the standard software packages PGOPHER⁴⁹ and Pickett's SPFIT/SPCAT suite.⁵⁰ Molecular parame-

Table 3: Calculated, best estimate (BE) and experimental molecular parameters of NCCO^+ in the ground vibrational and ν_2 excited states (in MHz, unless noted otherwise).

Parameter	Calc ^a	BE ^b	IR	mmw	IR & mmw
B_e	4554.302
ΔB_0	-5.819
B_0	4560.121	4564.6	4563.775(43)	4563.77641(15)	4563.77641(15)
$D \times 10^3$ ^c	0.537	0.592	0.603(26)	0.60956(14)	0.60956(14)
α_2	17.002	17.07	17.0746(19)	...	17.0745(19)
$\tilde{\nu}_2 / \text{cm}^{-1}$	2149.3	2152	2149.64318(4)	...	2149.64318(4)
$eQq(\text{N})$	-5.880	-5.827
$rms_{\text{IR}} \times 10^4 / \text{cm}^{-1}$	2.0	...	2.0
$rms_{\text{mmw}} \times 10^3$	7.7	7.7

^a B_e and $eQq(\text{N})$ calculated at the ae-CCSD(T)/cc-pwCVQZ level; ΔB_0 , D , α_2 , and $\tilde{\nu}_2$ calculated at the fc-CCSD(T)/ANO2 level.

^b BE values derived from using NCCN as calibrator except for $eQq(\text{N})$ that was scaled using NCCNH^+ , see text for details.

^c Calculation yields equilibrium value, $D = D_e$; In the IR and global fits, a common constant has been used for both states, $D = D_0 = D_2$.

ters obtained from a fit to all rotational-vibrational lines using a standard linear molecule Hamiltonian are summarized in Table 3. With only four parameters varied in the fit – the ground vibrational-state constant B_0 , the rotation-vibration interaction constant α_2 , a common centrifugal distortion constant D for both vibrational states and the vibrational band center $\tilde{\nu}_2$ – the data are reproduced to within an rms of $2 \times 10^{-4} \text{ cm}^{-1}$. Very good agreement between the experimental (column 'IR' in Table 3) and the calculated rotational constants (column 'Calc') is observed with deviations not exceeding 3.7 MHz (0.08%). The difference between the experimental and calculated vibrational wavenumber is very small also, 0.3 cm^{-1} or 0.02%. The agreement between the experimental ground state rotational constant and the corresponding best estimate value (column 'BE') is even better ($< 1 \text{ MHz}$, 0.02%). While for scaling purposes to arrive at a NCCO^+ BE value of B_0 structurally very closely related cyanogen, NCCN, was used initially (Table 3), the approach has also been tested on an extended sample of ten isoelectronic (and hence potentially applicable) calibrators known from previous experiment (cf., section “Quantum-chemical calculations” and Supporting Information). In this effort, equilibrium rotational constants B_e were calculated at the ae-

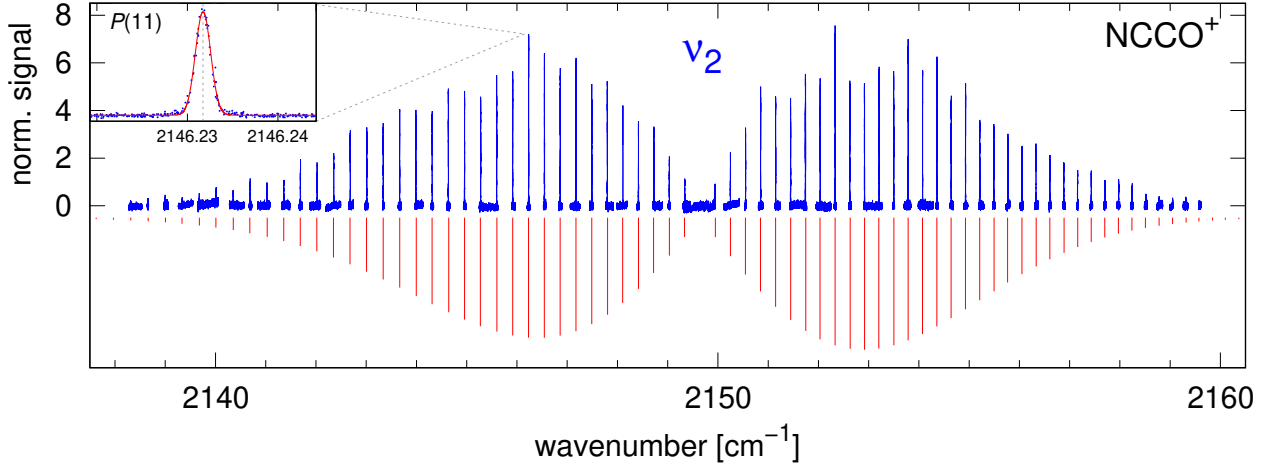


Figure 4: LO spectrum of the ν_2 stretching mode of bare NCCO^+ (blue trace) recorded at a nominal trap temperature of 42(2) K using 10^{12} cm^{-3} of N_2 as a neutral collision partner. Normalized signal is plotted against the wavenumber. A simulation of the rotational-vibrational lines assuming a rotational temperature of 50 K is shown for comparison as inverted red sticks. An enlarged view of the $P(11)$ transition is shown in the top left corner.

CCSD(T)/cc-pwCVQZ level and, for practical reasons, zero-point vibrational contributions ΔB_0 were computed at the more affordable fc-CCSD(T)/ANO1 level of theory. Scaling factors derived from the ratios $B_{0,exp}/B_{0,calc}$ in this fashion are very similar (~ 1.001) and invariably result in BE values that represent a significant improvement over the calculated B_0 of NCCO^+ alone ($|B_{0,BE} - B_{0,IR}| \leq 1 \text{ MHz}$, see Supporting Information). This finding highlights that empirical scaling may be a worthwhile and potentially very inexpensive approach for effectively improving computational results as long as at least one isoelectronic and isostructural molecule is known from previous high-resolution study.

NCCO⁺ pure rotational spectrum

Based on the molecular data obtained in the high-resolution study of the ν_2 vibrational mode, the pure rotational spectrum of NCCO^+ was finally studied using a LO-IR/mmw double resonance approach used recently with very good success in studies of other molecular ions.^{6,51–55} For this purpose, the IR laser is constantly kept fixed on the center frequency of a ro-vibrational transition while the millimeter-wave source is tuned in a region centered at

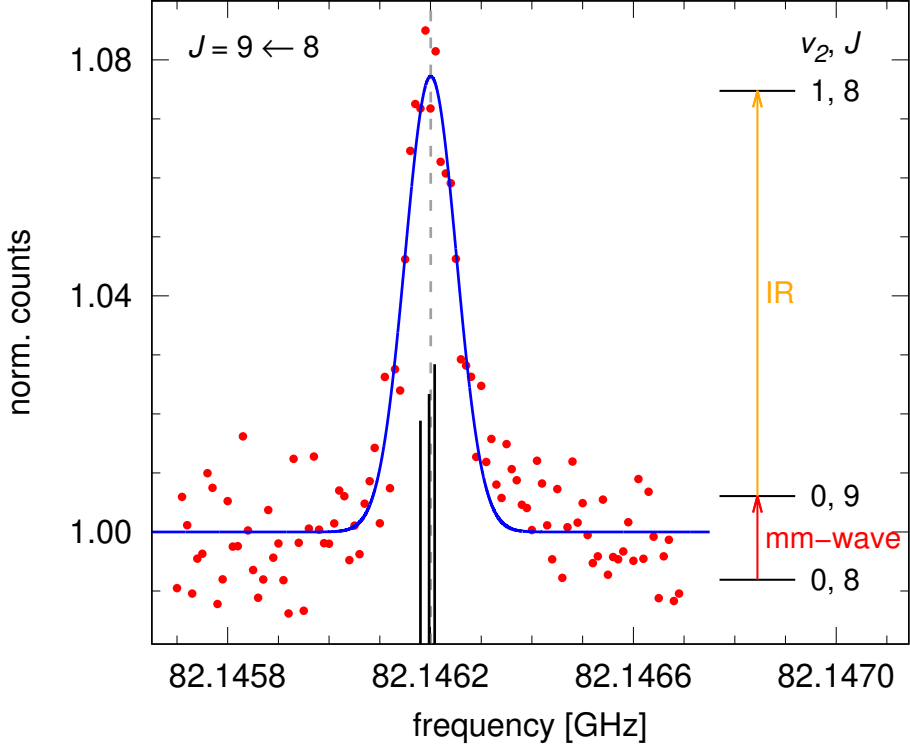


Figure 5: Pure rotational transition $J = 9 \leftarrow 8$ in the ground vibrational state of NCCO^+ , recorded using a LO IR/mmwave double resonance scheme. For this recording, the IR laser was stabilized on the $P(9)$ transition of the ν_2 vibrational mode (orange arrow) while tuning the mmwave source in steps of 10 kHz around the predicted frequency of 82.146 GHz. Here, resonant mmwave excitation (red arrow) results in an increase of the LO signal of about 8%. Normalized counts (red dots) are determined from the ratio of the ion counts in the mmwave search window and the counts determined at an off-resonant reference frequency. Calculated quadrupole hyperfine structure from nitrogen is indicated as black sticks.

the predicted rotational transition frequency. By changing the population of the lower level of the infrared transition through resonant rotational excitation, a change in the LOS signal may be detected. An example of this approach is given in Fig. 5 that shows the $J = 9 \leftarrow 8$ rotational transition of NCCO^+ , detected through monitoring the $P(9)$ LO signal and tuning the millimeter-wave source in the region between 82145.7 MHz and 82146.7 MHz. The counts (red dots) were determined by averaging the counts of several up and down scans. Overall, using this DR technique a total of sixteen rotational transitions of NCCO^+ were measured covering rotational angular momentum quantum numbers $8 \leq J'' \leq 26$, except $J'' = 15$ and 16 (Table 4 and Fig. S7). The experimental data are well described by a Gaussian line

profile indicating a thermal ensemble. From a fit of the rotational transition frequencies, the B_0 and D_0 ground state rotational parameters have been determined to much higher precision than from the high-resolution infrared data of the ν_2 mode (Table 3). The mmw fit *rms* obtained is 8 kHz and hence only a very small fraction of the line widths of a few hundred kHz. Since the line widths show a significant dependence on the mmw-power used, indicating power broadening effects, the experimental conditions were chosen to achieve an optimal balance between intensity and width. No hyperfine structure from the presence of the ^{14}N nucleus ($I = 1$) was spectroscopically resolved in the pure rotational spectra (see Fig. 5). However, an accurate quadrupole coupling parameter is obtained from calculations; at the ae-CCSD(T)/cc-pwCVQZ level, this amounts to $eQq = -5.880$ MHz. It turns out that this value is very similar to the corresponding one found for the terminal nitrogen nucleus in the NCCNH^+ molecular ion ($-5.480(3)$ MHz) with Fourier transform microwave spectroscopy,⁴² an indication that the nitrogen nuclei share a very similar electronic environment in both ions. Empirical scaling using an ae-CCSD(T)/cc-pwCVQZ structural calculation of NCCNH^+ results in a corrections factor $eQq_{exp}/eQq_{calc} = -5.480/ - 5.532$ close to unity and hence a very small impact on the predicted eQq_{calc} of NCCO^+ . The BE value obtained in this fashion is -5.827 MHz and should permit very accurate predictions of the quadrupole hyperfine structure in the rotational spectrum of NCCO^+ , in particular for low- J transitions where the strong $\Delta F = +1$ components might be resolvable.

Conclusions and Outlook

This paper reports on the first spectroscopic detection and characterization of the linear NCCO^+ ion, achieved by employing highly sensitive action spectroscopic methods in cryogenic ion trap apparatus. Initial spectroscopic detection was accomplished using IRPD spectroscopy of the weakly bound $\text{NCCO}^+ - \text{Ne}$ cluster followed-up upon by high-resolution IR-LOS of the ν_2 fundamental of bare NCCO^+ and concluded with LO IR/mmw double

Table 4: Rotational transition frequencies of NCCO^+ in the ground vibrational state (in MHz) and fit residuals $o - c$ (kHz).

$J' \leftarrow J''$	Experimental	$o - c$
$9 \leftarrow 8$	82146.1978	-0.2
$10 \leftarrow 9$	91273.0957	5.7
$11 \leftarrow 10$	100399.8551	19.3
$12 \leftarrow 11$	109526.4239	3.3
$13 \leftarrow 12$	118652.8269	-3.0
$14 \leftarrow 13$	127779.0479	-1.2
$18 \leftarrow 17$	164281.7258	-5.3
$19 \leftarrow 18$	173406.7764	-3.5
$20 \leftarrow 19$	182531.5372	-13.5
$21 \leftarrow 20$	191656.0360	7.1
$22 \leftarrow 21$	200780.1894	-10.5
$23 \leftarrow 22$	209904.0435	-5.6
$24 \leftarrow 23$	219027.5667	5.0
$25 \leftarrow 24$	228150.7249	1.6
$26 \leftarrow 25$	237273.5280	8.8
$27 \leftarrow 26$	246395.9347	0.1

resonance spectroscopy of 16 pure rotational transitions between 82 and 247 GHz. Based on the experimental and calculated molecular parameters, the rotational spectrum of NCCO^+ in its ground vibrational state can now be predicted accurately from the microwave well into the submillimeter-wave range, a prerequisite for dedicated and sensitive radio astronomical searches. Although NCCO^+ is not currently included in standard astrochemical models,^{56,57} its close structural and compositional similarity to known astronomical species makes it an attractive candidate for future astronomical searches. Frequency predictions will be provided through a corresponding entry in the Cologne Database for Molecular spectroscopy.^{1,58}

Besides high-resolution characterization of other vibrational bands of NCCO^+ such as the strong ν_1 mode at 2340 cm^{-1} , future extension towards spectroscopic characterization of other $[\text{2C,N,O}]^+$ structural isomers seems promising. Energetically, ground state NCCO^+ is followed by linear CNCO^+ calculated to lie only 11 kcal/mol above.¹² Some evidence for the production of CNCO^+ has been obtained already previously through mass spectrometry.⁸ By comparison, in the isoelectronic $[\text{2C,2N}]$ system, at least three structural isomers are

known spectroscopically, two by observations at high-resolution in the gas phase, cyanogen, NCCN,³⁵ and isocyanogen, CNCN³⁶ (located +26 kcal/mol above NCCN⁵⁹) and a third one, diisocyanogen, CNNC, trapped in a matrix of solid Ar at low temperatures⁶⁰ (+74 kcal/mol).

Laboratory studies of new thioacylium species, $R-CS^+$, in which the oxygen atom of acylium ions is replaced with isovalent sulfur would be another interesting area of research. No $[2C,N,S]^+$ species have yet been characterized spectroscopically, but calculations indicate linear $NCCS^+$ to represent the global minimum arrangement.⁶¹ In the present study, exploratory anharmonic fc-CCSD(T)/ANO2 calculations of $NCCS^+$ indicate the vibrational spectrum to be dominated by the strong C-N and C-S stretching fundamental bands located at 2175 cm^{-1} and 1630 cm^{-1} , respectively, and hence promising targets for future infrared studies. Also, at the ae-CCSD(T)/cc-pwCVQZ level, $NCCS^+$ is calculated to be very polar, with a center-of-mass dipole moment of 3.77 D and a rotational constant of about 2.8 GHz, making it an attractive candidate for studies of its pure rotational spectrum in the microwave region. Similar to the scaling approach performed for the HC_3S^+ molecular ion,³³ using isoelectronic NCCP⁶² for calibration purposes, should provide a rotational constant of very high accuracy, possibly as good as to within 1 MHz (cf. Refs. 33,63). It might be worthwhile to mention that the Fourier transform microwave spectrum of the kinked $NCCS$ radical has been known already for 20 years.⁶⁴

In summary, the present work demonstrates the power of action spectroscopy in cold ion traps where different variants are performed in a sequential fashion: Initially, the vibrational bands of target species are identified in low-resolution studies followed by investigations at high resolution unfolding their rotational substructures. Finally, pure rotational spectra may be recorded at even much higher resolution as needed for subsequent radio astronomical searches. The fast scanning speed of leak-out spectroscopy is unprecedented and will greatly support the study of many new ions of astrophysical interest in the future.

Conflicts of interest

There are no conflicts of interest to declare.

Acknowledgement

We are grateful to Prof. Dr. Britta Redlich for a generous donation of FELIX director's beamtime for the IRPD study, Radboud University, the Nederlandse Organisatie voor Wetenschappelijk Onderzoek (NWO) as well as the FELIX staff for support. This work has been supported by an ERC advanced grant (Missions: 101020583), by the Deutsche Forschungsgemeinschaft (DFG) via the Collaborative Research Centre 1601 (project ID: 500700252, sub-project B8 and C4) and the Gerätezentrum “Cologne Center for Terahertz Spectroscopy” (DFG SCHL 341/15-1). We thank Florian Pirlet for technical support and the Regional Computing Center of the Universität zu Köln (RRZK) for providing computing time on the DFG-funded high-performance computing system CHEOPS. The authors gratefully acknowledge the work carried out in recent years by the electrical and mechanical workshops of the I. Physikalisches Institut, without whose support the construction of the new ion trap apparatus COLtrap II would not have been possible.

Supporting Information Available

The Supporting Information is available free of charge providing further details on quantum-chemical calculations, the ion temperature, mass spectra, enlarged ro-vibrational spectra, IR linelist, and spectra of pure rotational transitions.

References

- (1) Müller, H. S. P.; Thorwirth, S.; Roth, D. A.; Winnewisser, G. The Cologne Database

for Molecular Spectroscopy, CDMS. *Astron. Astrophys.* **2001**, *370*, L49–L52.

(2) Buhl, D.; Snyder, L. E. Unidentified Interstellar Microwave Line. *Nature* **1970**, *228*, 267–269.

(3) Woods, R. C.; Dixon, T. A.; Saykally, R. J.; Szanto, P. G. Laboratory microwave spectrum of HCO^+ . *Phys. Rev. Lett.* **1975**, *35*, 1269–1272.

(4) Cernicharo, J.; Marcelino, N.; Agundez, M.; Endo, Y.; Cabezas, C.; Bermudez, C.; Tercero, B.; de Vicente, P. Discovery of HC_3O^+ in space: The chemistry of O-bearing species in TMC-1. *Astron. Astrophys.* **2020**, *642*, L17.

(5) Cernicharo, J.; Cabezas, C.; Bailleux, S.; Margules, L.; Motiyenko, R.; Zou, L.; Endo, Y.; Bermudez, C.; Agundez, M.; Marcelino, N. et al. Discovery of the acetyl cation, CH_3CO^+ , in space and in the laboratory. *Astron. Astrophys.* **2021**, *646*, L7.

(6) Asvany, O.; Thorwirth, S.; Schmid, P. C.; Salomon, T.; Schlemmer, S. High-resolution ro-vibrational and rotational spectroscopy of HC_3O^+ . *Phys. Chem. Chem. Phys.* **2023**,

(7) Pyykkö, P.; Runeberg, N. Ab initio studies of bonding trends. *J. Mol. Struct. (THEOCHEM)* **1991**, *234*, 269–277.

(8) McGibbon, G. A.; Kingsmill, C. A.; Terlouw, J. K.; Bergers, P. C. The isomeric C_2NO^+ ions NCCO^+ , CNCO^+ , CCNO^+ and their neutral counterparts are stable species in the gas-phase. *Int. J. Mass. Spectrom. Ion Proc.* **1992**, *121*, R11–R18.

(9) Francisco, J. S.; Liu, R. F. An ab initio study of OCCN and OCCN^+ . *J. Chem. Phys.* **1997**, *107*, 3840–3844.

(10) Jursic, B. S. Density functional theory investigation of physical properties of the OCCN radical and the cation. *J. Mol. Struct. (THEOCHEM)* **1999**, *460*, 207–212.

(11) Yu, G.-t.; Ding, Y.-h.; Huang, X.-r.; Bai, H.-t.; Sun, C.-c. Theoretical Study on Stability and Properties of NC_2O Isomers. *J. Phys. Chem. A* **2005**, *109*, 2364–2372.

(12) Chi, Y.-j.; Yu, H.-t. Looking for the stable isomers of $[\text{N,C,C,O}]^+$ system. *J. Mol. Struct. (THEOCHEM)* **2006**, *763*, 91 – 96.

(13) Oepts, D.; van der Meer, A. F. G.; van Amersfoort, P. W. The Free-Electron-Laser user facility FELIX. *Infrared Phys. Technol.* **1995**, *36*, 297–308.

(14) Jusko, P.; Brünken, S.; Asvany, O.; Thorwirth, S.; Stoffels, A.; van der Meer, L.; Berden, G.; Redlich, B.; Oomens, J.; Schlemmer, S. The FELion cryogenic ion trap beam line at the FELIX free-electron laser laboratory: Infrared signatures of primary alcohol cations. *Faraday Discuss.* **2019**, *217*, 172–202.

(15) Asvany, O.; Bielau, F.; Moratschke, D.; Krause, J.; Schlemmer, S. New design of a cryogenic linear RF multipole trap. *Rev. Sci. Instr.* **2010**, *81*, 076102.

(16) Bast, M.; Böing, J.; Salomon, T.; Thorwirth, S.; Asvany, O.; Schäfer, M.; Schlemmer, S. Ro-vibrational spectra of C-C stretching modes of C_3H^+ and HC_3O^+ . *J. Mol. Spectrosc.* **2023**, *398*, 111840.

(17) Schmid, P. C.; Asvany, O.; Salomon, T.; Thorwirth, S.; Schlemmer, S. Leak-Out Spectroscopy, A Universal Method of Action Spectroscopy in Cold Ion Traps. *J. Phys. Chem. A* **2022**, *126*, 8111–8117.

(18) Jusko, P.; Asvany, O.; Wallerstein, A.-C.; Brünken, S.; Schlemmer, S. Two-Photon Rotational Action Spectroscopy of Cold OH^- at 1 ppb Accuracy. *Phys. Rev. Lett.* **2014**, *112*, 253005–4.

(19) Raghavachari, K.; Trucks, G. W.; Pople, J. A.; Head-Gordon, M. A 5th-order perturbation comparison of electron correlation theories. *Chem. Phys. Lett.* **1989**, *157*, 479–483.

(20) Dunning, T. H. Gaussian basis sets for use in correlated molecular calculations. I. The atoms boron through neon and hydrogen. *J. Chem. Phys.* **1989**, *90*, 1007–1023.

(21) Kendall, R. A.; Dunning, T. H.; Harrison, R. J. Electron affinities of the first-row atoms revisited. Systematic basis sets and wave functions. *J. Chem. Phys.* **1992**, *96*, 6796–6806.

(22) Woon, D. E.; Dunning, T. H. Gaussian basis sets for use in correlated molecular calculations. III. The atoms aluminum through argon. *J. Chem. Phys.* **1993**, *98*, 1358–1371.

(23) Peterson, K. A.; Dunning, T. H. Accurate correlation consistent basis sets for molecular core-valence correlation effects: The second row atoms Al–Ar and the first row atoms B–Ne revisited. *J. Chem. Phys.* **2002**, *117*, 10548–10560.

(24) Almlöf, J.; Taylor, P. R. General contraction of Gaussian basis sets. I. Atomic natural orbitals for 1st-row and 2nd-row atoms. *J. Chem. Phys.* **1987**, *86*, 4070–4077.

(25) Watts, J. D.; Gauss, J.; Bartlett, R. J. Open-shell analytical energy gradients for triple excitation many-body, coupled-cluster methods - MBPT(4), CCSD+T(CCSD), CCSD(T), and QCISD(T). *Chem. Phys. Lett.* **1992**, *200*, 1–7.

(26) Gauss, J.; Stanton, J. F. Analytic CCSD(T) second derivatives. *Chem. Phys. Lett.* **1997**, *276*, 70–77.

(27) Stanton, J. F.; Gauss, J. Analytic second derivatives in high-order many-body perturbation and coupled-cluster theories: computational considerations and applications. *Int. Rev. Phys. Chem.* **2000**, *19*, 61–95.

(28) Mills, I. M. In *Molecular Spectroscopy: Modern Research*; Rao, K. N., Mathews, C. W., Eds.; Academic Press: New York, 1972; pp 115–140.

(29) Stanton, J. F.; Lopreore, C. L.; Gauss, J. The equilibrium structure and fundamental vibrational frequencies of dioxirane. *J. Chem. Phys.* **1998**, *108*, 7190–7196.

(30) Stanton, J. F.; Gauss, J.; Cheng, L.; Harding, M. E.; Matthews, D. A.; Szalay, P. G. CFOUR, Coupled-Cluster techniques for Computational Chemistry, a

quantum-chemical program package. With contributions from A. Asthana, A.A. Auer, R.J. Bartlett, U. Benedikt, C. Berger, D.E. Bernholdt, S. Blaschke, Y. J. Bomble, S. Burger, O. Christiansen, D. Datta, F. Engel, R. Faber, J. Greiner, M. Heckert, O. Heun, M. Hilgenberg, C. Huber, T.-C. Jagau, D. Jonsson, J. Jusélius, T. Kirsch, M.-P. Kitsaras, K. Klein, G.M. Kopper, W.J. Lauderdale, F. Lipparini, J. Liu, T. Metzroth, L. Monzel, L.A. Mück, D.P. O'Neill, T. Nottoli, J. Oswald, D.R. Price, E. Prochnow, C. Puzzarini, K. Ruud, F. Schiffmann, W. Schwalbach, C. Simmons, S. Stopkowicz, A. Tajti, T. Uhlířová, J. Vázquez, F. Wang, J.D. Watts, P. Yergün, C. Zhang, X. Zheng, and the integral packages MOLECULE (J. Almlöf and P.R. Taylor), PROPS (P.R. Taylor), ABACUS (T. Helgaker, H.J. Aa. Jensen, P. Jørgensen, and J. Olsen), and ECP routines by A. V. Mitin and C. van Wüllen. For the current version, see <http://www.cfour.de>.

- (31) Harding, M. E.; Metzroth, T.; Gauss, J.; Auer, A. A. Parallel calculation of CCSD and CCSD(T) analytic first and second derivatives. *J. Chem. Theory Comput.* **2008**, *4*, 64–74.
- (32) Martinez, Jr., O.; Lattanzi, V.; Thorwirth, S.; McCarthy, M. C. Detection of protonated vinyl cyanide, $\text{CH}_2\text{CHCNH}^+$, a prototypical branched nitrile cation. *J. Chem. Phys.* **2013**, *138*, 094316.
- (33) Thorwirth, S.; Harding, M. E.; Asvany, O.; Brünken, S.; Jusko, P.; Lee, K. L. K.; Salomon, T.; McCarthy, M. C.; Schlemmer, S. Descendant of the X-ogen carrier and a ‘mass of 69’: infrared action spectroscopic detection of HC_3O^+ and HC_3S^+ . *Mol. Phys.* **2020**, *118*, e1776409.
- (34) Cabezas, C.; Agúndez, M.; Marcelino, N.; Tercero, B.; Fuentetaja, R.; de Vicente, P.; Cernicharo, J. Discovery of a new molecular ion, HC_7NH^+ , in TMC-1. *Astron. Astrophys.* **2022**, *659*, L8.

(35) Maki, A. G. High-resolution infrared spectrum of cyanogen. *J. Mol. Spectrosc.* **2011**, *269*, 166–174.

(36) Gerry, M. C. L.; Stroh, F.; Winnewisser, M. The microwave Fourier transform, millimeter-wave, and submillimeter-wave rotational spectra of isocyanogen, CNCN. *J. Mol. Spectrosc.* **1990**, *140*, 147–161.

(37) Bizzocchi, L.; Degli Esposti, C.; Dore, L. Accurate rest frequencies for the submillimetre-wave lines of C₃O in ground and vibrationally excited states below 400 cm⁻¹. *Astron. Astrophys.* **2008**, *492*, 875–881.

(38) Amano, T. Submillimeter-wave spectrum of C₃N⁻ in the extended negative glow and hollow-anode discharges. *J. Mol. Spectrosc.* **2010**, *259*, 16–19.

(39) Amano, T. Extended negative glow and “hollow anode” discharges for submillimeter-wave observation of CN⁻, C₂H⁻, and C₄H⁻. *J. Chem. Phys.* **2008**, *129*, 244305.

(40) Thorwirth, S.; Müller, H. S. P.; Winnewisser, G. The Millimeter- and Submillimeter-Wave Spectrum of HC₃N in the Ground and vibrationally Excited States. *J. Mol. Spectrosc.* **2000**, *204*, 133–144.

(41) Guarnieri, A.; Hinze, R.; Krüger, M.; Zerbe-Foese, H.; Lentz, D.; Preugschat, D. The millimeter-wave spectrum of ethynylisocyanide (HCCNC). *J. Mol. Spectrosc.* **1992**, *156*, 39–47.

(42) Gottlieb, C. A.; Apponi, A. J.; McCarthy, M. C.; Thaddeus, P.; Linnartz, H. The rotational spectra of the H₃CCNH⁺, NCCNH⁺, and CH₃CNH⁺ ions. *J. Chem. Phys.* **2000**, *113*, 1910–1915.

(43) Agúndez, M.; Cabezas, C.; Marcelino, N.; Fuentetaja, R.; Tercero, B.; de Vicente, P.; Cernicharo, J. A new protonated molecule discovered in TMC-1: HCCNCH⁺. *Astron. Astrophys.* **2022**, *659*, L9.

(44) Thorwirth, S.; Steenbakkers, K.; Danowski, T.; Schmid, P. C.; Bonah, L.; Asvany, O.; Brünken, S.; Schlemmer, S. Gas-Phase Infrared Action Spectroscopy of CH_2Cl^+ and CH_3ClH^+ : Likely Protagonists in Chlorine Astrochemistry. *Molecules* **2024**, *29*, 665.

(45) Bak, K. L.; Gauss, J.; Jørgensen, P.; Olsen, J.; Helgaker, T.; Stanton, J. F. The accurate determination of molecular equilibrium structures. *J. Chem. Phys.* **2001**, *114*, 6548–6556.

(46) Coriani, S.; Marchesan, D.; Gauss, J.; Hättig, C.; Helgaker, T.; Jørgensen, P. The accuracy of ab initio molecular geometries for systems containing second-row atoms. *J. Chem. Phys.* **2005**, *123*, 184107.

(47) Pivonka, N. L.; Kaposta, C.; Brümmer, M.; von Helden, G.; Meijer, G.; Wöste, L.; Neumark, D. M.; Asmis, K. R. Probing a strong hydrogen bond with infrared spectroscopy: Vibrational predissociation of $\text{BrHBr}^-\cdot\text{Ar}$. *J. Chem. Phys.* **2003**, *118*, 5275–5278.

(48) Brünken, S.; Lipparini, F.; Stoffels, A.; Jusko, P.; Redlich, B.; Gauss, J.; Schlemmer, S. Gas-Phase Vibrational Spectroscopy of the Hydrocarbon Cations $\text{l-C}_3\text{H}^+$, HC_3H^+ , and $\text{c-C}_3\text{H}_2^+$: Structures, Isomers, and the Influence of Ne-Tagging. *J. Phys. Chem. A* **2019**, *123*, 8053–8062.

(49) Western, C. M. PGOPHER: A program for simulating rotational, vibrational and electronic spectra. *J. Quant. Spectrosc. Radiat. Transfer* **2016**, *186*, 221–241.

(50) Pickett, H. M. The fitting and prediction of vibration-rotation spectra with spin interactions. *J. Mol. Spectrosc.* **1991**, *148*, 371–377.

(51) Gupta, D.; Silva, W. G. D. P.; Doménech, J. L.; Plaar, E.; Thorwirth, S.; Schlemmer, S.; Asvany, O. High-resolution rovibrational and rotational spectroscopy of the singly deuterated cyclopropenyl cation, $\text{c-C}_3\text{H}_2\text{D}^+$. *Faraday Discuss.* **2023**, *245*, 298–308.

(52) Silva, W. G. D. P.; Cernicharo, J.; Schlemmer, S.; Marcelino, N.; Loison, J.-C.; Agúndez, M.; Gupta, D.; Wakelam, V.; Thorwirth, S.; Cabezas, C. et al. Discovery of H₂CCCH⁺ in TMC-1. *Astron. Astrophys.* **2023**, *676*, L1.

(53) Silva, W. G. D. P.; Gupta, D.; Plaar, E.; Doménech, J. L.; Schlemmer, S.; Asvany, O. High resolution rovibrational and rotational spectroscopy of H₂CCCH⁺. *Mol. Phys.* **2024**, *122*, e2296613.

(54) Silva, W. G. D. P.; Bonah, L.; Schmid, P. C.; Schlemmer, S.; Asvany, O. Hyperfine-resolved rotational spectroscopy of HCNH⁺. *J. Chem. Phys.* **2024**, *160*, 071101.

(55) Baddeliyanage, C.; Karner, J.; Melath, S. P.; Silva, W. G.; Schlemmer, S.; Asvany, O. Extending the laboratory rotational spectrum of linear C₃H⁺. *J. Mol. Spectrosc.* **2025**, *407*, 111978.

(56) Wakelam, V.; Herbst, E.; Loison, J.-C.; Smith, I. W. M.; Chandrasekaran, V.; Pavone, B.; Adams, N. G.; Bacchus-Montabonel, M.-C.; Bergeat, A.; Béroff, K. et al. A kinetic database for astrochemistry (KIDA). *Astrophys. J. Suppl. Ser.* **2012**, *199*, 21.

(57) Millar, T. J.; Walsh, C.; Van de Sande, M.; Markwick, A. J. The UMIST Database for Astrochemistry 2022. *Astron. Astrophys.* **2024**, *682*, A109.

(58) Endres, C. P.; Schlemmer, S.; Schilke, P.; Stutzki, J.; Müller, H. S. P. The Cologne Database for Molecular Spectroscopy, CDMS, in the Virtual Atomic and Molecular Data Centre, VAMDC. *J. Mol. Spectrosc.* **2016**, *327*, 95–104.

(59) Ding, Y. H.; Huang, X. R.; Li, Z. S.; Sun, C. C. Theoretical study on potential-energy surface of C₂N₂. *J. Chem. Phys.* **1998**, *108*, 2024–2027.

(60) Maier, G.; Reisenauer, H. P.; Eckwert, J.; Sierakowski, C.; Stumpf, T. Matrix Isolation of Diisocyanogen CNNC. *Angew. Chem. Int. Ed. Engl.* **1992**, *31*, 1218–1220.

(61) Chi, Y.-j.; Yu, H.-t. Structure and stability of the $[\text{N},\text{C},\text{C},\text{S}]^+$ system isomers. *Journal of Molecular Structure: THEOCHEM* **2006**, *766*, 165–167.

(62) Bizzocchi, L.; Thorwirth, S.; Müller, H. S. P.; Lewen, F.; Winnewisser, G. Submillimeter-Wave Spectroscopy of Phosphaalkynes: HCCCP, NCCP, HCP, and DCP. *J. Mol. Spectrosc.* **2001**, *205*, 110–116.

(63) Cernicharo, J.; Cabezas, C.; Endo, Y.; Marcelino, N.; Agundez, M.; Tercero, B.; Gallego, J. D.; de Vicente, P. Space and laboratory discovery of HC_3S^+ . *Astron. Astrophys.* **2021**, *646*, L3.

(64) McCarthy, M. C.; Cooksy, A. L.; Mohamed, S.; Gordon, V. D.; Thaddeus, P. Rotational Spectra of the Nitrogen-Sulfur Carbon Chains NC_nS , $n = 1 - 7$. *Astrophys. J. Suppl. Ser.* **2003**, *144*, 287–297.

TOC Graphic

